Allosteric modulation of Ca^{2+} channels by G proteins, voltage-dependent facilitation, protein kinase C, and $Ca_v\beta$ subunits

Stefan Herlitze*, Huijun Zhong, Todd Scheuer, and William A. Catterall†

Department of Pharmacology, Mail Stop 357280, University of Washington, Seattle, WA 98195-7280

Contributed by William A. Catterall, December 28, 2000

N-type and P/Q-type Ca^{2+} channels are inhibited by neurotransmitters acting through G protein-coupled receptors in a membrane-delimited pathway involving $G\beta\gamma$ subunits. Inhibition is caused by a shift from an easily activated ''willing'' (*W*) state to a more-difficult-to-activate ''reluctant'' (*R*) state. This inhibition can be reversed by strong depolarization, resulting in prepulse facilitation, or by protein kinase C (PKC) phosphorylation. Comparison of regulation of N-type Ca^{2+} channels containing Cav2.2a α_1 subunits and P/Q-type Ca^{2+} channels containing $Ca_v2.1$ α_1 subunits revealed substantial differences. In the absence of G protein modulation, $Ca_v2.1$ channels containing $Ca_v\beta$ subunits were tonically in the *W* state, whereas $Ca_v2.1$ channels without β subunits and $Ca_v2.2a$ channels with β subunits were tonically in the *R* state. Both $Ca_v2.1$ and $Ca_v2.2a$ channels could be shifted back toward the *W* state by strong depolarization or PKC phosphorylation. Our results show that the *R* state and its modulation by prepulse facilitation, PKC phosphorylation, and $Ca_v\beta$ subunits are intrinsic properties of the Ca^{2+} channel itself in the absence of G protein modulation. A common allosteric model of G protein modulation of Ca^{2+}-channel activity incorporating an intrinsic equilibrium between the *W* and *R* states of the α_1 subunits and modulation of that equilibrium by G proteins, $Ca_v\beta$ subunits, membrane depolarization, and phosphorylation by PKC accommodates our findings. Such regulation will modulate transmission at synapses that use N-type and P/Q-type Ca^{2+} channels to initiate neurotransmitter release.

neuromodulation | calcium channels | $G\beta\gamma$ subunits | protein phosphorylation

Neuronal voltage-gated Ca^{2+} channels are involved in multiple cellular functions including neurotranstransmitter release, Ca^{2+}-mediated regulatory processes, and generation of dendritic action potentials. Electrophysiological and pharmacological studies distinguish at least six classes of Ca^{2+} currents designated L-, N-, P-, Q-, R-, and T-type (1, 2). Ca^{2+} channels consist of complexes of a pore-forming α_1 subunit with $\alpha_2\delta$, β, and γ subunits (2, 3). Ca^{2+} channels containing $Ca_v2.2$ α_1 subunits (formerly α_{1B}; ref. 4) are responsible for N-type currents, and Ca^{2+} channels containing $Ca_v2.1$ α_1 subunits (formerly α_{1A}; ref. 4) are responsible for both P- and Q-type Ca^{2+} currents (5–10). The $Ca_v2.1$ and $Ca_v2.2$ channels are located in presynaptic nerve terminals (10–13) and are responsible for the Ca^{2+} entry that triggers neurotransmitter release at most synapses (14, 15).

These two channel types are inhibited by neurotransmitter receptors acting through pertussis toxin-sensitive G proteins via membrane-delimited pathways that cause a positive shift in the voltage dependence of channel activation (16–18). This inhibition can be reversed by strong depolarization leading to prepulse facilitation of Ca^{2+} currents (19–22). The effect of G proteins has been modeled as a shift in channel state from a ''willing'' (*W*) state, in which activation occurs rapidly at relatively negative membrane potentials, to a ''reluctant'' (*R*) state, in which activation is slower and requires stronger depolarization (16). G-protein modulation is mediated by $G\beta\gamma$ subunits (23, 24) in part through direct binding to a site in the intracellular loop connecting domains I and II of the α_1 subunit of the Ca^{2+} channel (25–28). N-type and P/Q-type Ca^{2+} channels are regulated also by protein kinase C (PKC). PKC can increase the activity of N-type and P/Q-type Ca^{2+} channels directly (29) and also can reverse their inhibition by G proteins (30, 31) by phosphorylating site(s) in the intracellular loop connecting domains I and II (28, 32). Such modulation of Ca^{2+} channels is thought to influence the efficiency of synaptic transmission strongly (17).

We have expressed specific isoforms of $Ca_v2.1$ and $Ca_v2.2$ channels in the human embryonic kidney cell line tsA-201 and analyzed their function, regulation by G proteins, facilitation by depolarizing prepulses, and modulation by PKC. Our results reveal surprising differences in modulation of these two channel types and suggest a common allosteric mechanism for Ca^{2+}-channel modulation by these diverse regulatory pathways.

NEUROBIOLOGY

Experimental Procedures

cDNAs encoding $\alpha_1$2.1 (rbA isoform; ref. 33), $\alpha_1$2.2a (rbB-I isoform; ref. 5) and β1b were cloned in pMT2XS (34), $\alpha_2\delta$ (35) in pZEM228, and CD8 in EBO-pcD. tsA-201 cells were transfected with the α_1, $\alpha_2\delta$, and β cDNAs in 1:1:1 molar ratios plus CD8 by using either calcium phosphate or Lipofectamine (Stratagene) and incubated for at least 48 h. Positively transfected cells were identified by labeling with anti-CD8 antibody tagged with fluorophore and analyzed by whole-cell patch clamp as described (24, 36). Currents were recorded and filtered at 10 kHz with an eight-pole Bessel filter. Leak and capacitative currents were measured and subtracted using the P/-4 method. Cells were bathed in an external solution containing 100 mM Tris, 4 mM $MgCl_2$, and 10 mM $BaCl_2$ with pH adjusted to 7.3 with methanesulfonic acid. The internal pipette solution consisted of 120 mM aspartic acid, 5 mM $CaCl_2$, 2 mM $MgCl_2$, 10 mM Hepes, 10 mM EGTA, and 2 mM Mg-ATP with pH adjusted to 7.3 with CsOH. When indicated in the figure legends, GTPγS was added to the internal solution at a concentration of 0.6 mM. 1-oleoyl-2-acetyl glycerol (OAG) was prepared as a 2-mM stock in DMSO. Cells were preincubated with 20 μM OAG for 2–4 h before recording. Recordings were performed in the absence of added OAG. Experiments describing the voltage dependencies were fit with Boltzmann relationships of the form $100\%/\{1 + \exp[(V - V_x)/k]\}$, in which V_x is the voltage of half activation (V_a), inactivation (V_h), or prepulse facilitation (V_f), and k is a slope factor.

Abbreviations: *W*, willing; *R*, reluctant; PKC, protein kinase C; OAG, 1-oleoyl-2-acetyl; IP, inhibitor peptide.

*Present address: Department of Neuroscience, Case Western Reserve University, Cleveland, OH 44106-4975.

†To whom reprint requests should be addressed. E-mail: wcatt@u.washington.edu.

The publication costs of this article were defrayed in part by page charge payment. This article must therefore be hereby marked "*advertisement*" in accordance with 18 U.S.C. §1734 solely to indicate this fact.

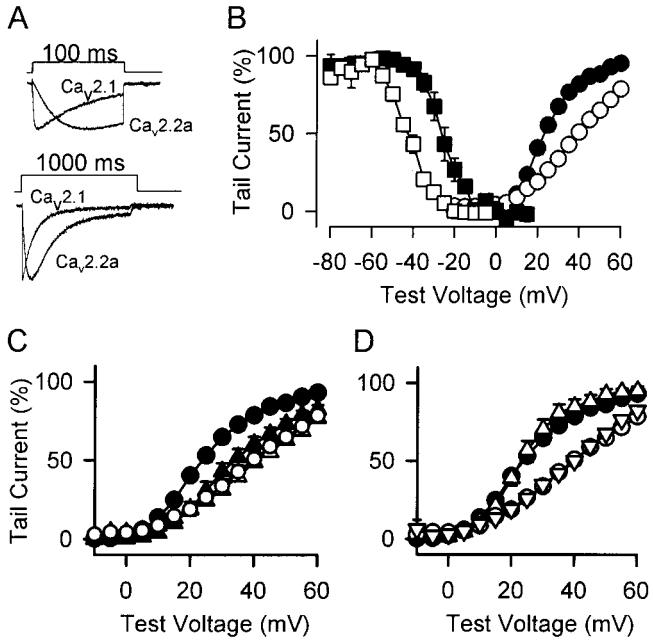

Fig. 1. Voltage-dependent activation and inactivation of the $Ca_v2.1$ and $Ca_v2.2a$ Ca^{2+} channels. (*A*) Rates of activation and inactivation. Ba^{2+} currents were recorded during 100-ms (*Upper*) or 1,000-ms (*Lower*) pulses to +30 mV from holding potentials of −60 mV ($Ca_v2.1$) or −70 mV ($Ca_v2.2a$). (*B*) Voltage dependence of activation and inactivation. To measure activation, tail currents were recorded at a holding potential of −60 mV ($Ca_v2.1$) or −70 mV ($Ca_v2.2a$) after a 4-ms ($Ca_v2.1$) or 50-ms ($Ca_v2.2a$) test pulse to the indicated potential. Means ± SEM of normalized tail currents were plotted as a function of the test voltage. ●, $Ca_v2.1$; ○, $Ca_v2.2a$. To measure inactivation, tail currents were recorded after a 4-s prepulse to the indicated potential followed by a 4-ms ($Ca_v2.1$) or 10-ms ($Ca_v2.2a$) test pulse to +30 mV. Means ± SEM of normalized tail currents were plotted as a function of prepulse voltage. ■, $Ca_v2.1$; □, $Ca_v2.2a$. (*C*) Voltage dependence of activation in the presence of intracellular GTPγS. ▲, $Ca_v2.1$; △, $Ca_v2.2a$. Results for activation of $Ca_v2.1$ (●) and $Ca_v2.2a$ (○) in the absence of GTPγS are replotted from *B* for comparison. (*D*) Voltage dependence of activation in the absence and presence of intracellular GDPβS for $Ca_v2.1$ (●, control; △, GDPβS) and $Ca_v2.2a$ (○, control; ▽, GDPβS).

Results

Voltage-Dependent Gating of Expressed P/Q-Type and N-Type Ca^{2+} Channels. P/Q-type Ca^{2+} channels composed of $\alpha_1$2.1, $\alpha_2\delta$, and β1b subunits and N-type Ca^{2+} channels composed of $\alpha_1$2.2a, $\alpha_2\delta$, and β1b subunits were expressed in the human embryonic kidney cell line tsA-201, and Ba^{2+} currents were measured in the whole-cell voltage-clamp configuration. Activation and inactivation kinetics during a test pulse to +30 mV are much slower for $Ca_v2.2a$ than for $Ca_v2.1$ (Fig. 1*A*). $Ca_v2.2a$ inactivates with a time constant of 313 ± 28 ms, whereas $Ca_v2.1$ exhibits a time constant of 127 ± 24 ms for inactivation (Fig. 1*A*). The voltage dependence of activation of $Ca_v2.2a$ is more positive (V_a = 42.2 mV) and more shallow than for $Ca_v2.1$ (V_a = 23.6 mV; Fig. 1*B*, ○ and ●). Steady-state inactivation from closed states during a 4-s conditioning pulse was observed at more-negative potentials (V_h = −41.5 ± 0.42 mV) for $Ca_v2.2a$ than for $Ca_v2.1$ (V_h = −25.4 ± 2.2 mV; Fig. 1*B*). Thus, these two channel types differ markedly in both activation and inactivation behavior.

G Protein Modulation. In the presence of GTPγS in the intracellular solution to activate G proteins, the voltage dependence of activation of $Ca_v2.1$ was shifted positively and was less steep than in control intracellular solution (Fig. 1*C*, compare ▲ with ●), reflecting inhibition of the Ca^{2+} channel by $G\beta\gamma$ caused by transition to the reluctant (*R*) state. In contrast, the voltage dependence of activation of $Ca_v2.2a$ channels was unaffected by GTPγS (Fig. 1*C*, compare ○ with △). Under GTPγS-modulated conditions, the voltage dependence of activation of $Ca_v2.1$ was comparable to that of $Ca_v2.2a$ channels without GTPγS (Fig. 1*C*, compare ▲ with ○). The positive value of V_a and the shallow voltage dependence of activation of $Ca_v2.2a$ suggest that it is tonically in the *R* state.

Because $Ca_v2.2a$ in the absence of GTPγS resembles a G protein-modulated Ca^{2+} channel in the *R* state, we investigated whether the G protein inhibitor GDPβS could cause a negative shift in the voltage dependence of activation. No significant difference in activation of $Ca_v2.1$ or $Ca_v2.2a$ was detected with 2 mM GDPβS in the intracellular solution (Fig. 1*D*), indicating that there was no tonic modulation of $Ca_v2.2a$ by activated G proteins in tsA-201 cells. Similarly, we found that the sulfhydryl agent *N*-ethyl maleimide, a selective inhibitor of G proteins, had no effect on these channels (ref. 37 and data not shown). These data support the conclusion that $Ca_v2.2a$ is tonically in the *R* state without G protein modulation, whereas $Ca_v2.1$ is tonically in the *W* state under basal conditions in tsA-201 cells.

Prepulse Facilitation. In many cell types, G protein-mediated effects on the Ca^{2+} current can be reversed by brief depolarizing prepulses, leading to prepulse facilitation (19–21). This reversal of G protein modulation is thought to reflect a shift of Ca^{2+} channels from the *R* to the *W* state induced by strong depolarization (16). To determine the facilitation properties of $Ca_v2.1$ and $Ca_v2.2a$, we examined the voltage dependence of activation in the absence or presence of a depolarizing prepulse to +100 mV (Fig. 2). In the presence of GTPγS, the Ba^{2+} currents through $Ca_v2.1$ are facilitated over a wide voltage range by depolarizing prepulses (Fig. 2*A*; ref. 24). The midpoint of the activation curve (V_a) of the facilitated current is shifted from 29.1 ± 3.5 mV to 18.6 ± 2.7 mV, and the facilitated activation curve is steeper than the control. Moreover, $Ca_v2.1$ activates more rapidly after a facilitating prepulse (Fig. 2*A*, *Inset*). These results are consistent with previous studies of G protein modulation and prepulse facilitation of P/Q-type Ca^{2+} channels in neurons (38, 39).

Surprisingly, although the expressed $Ca_v2.2a$ channels were unaffected by GTPγS and GDPβS (Fig. 1 *C* and *D*), striking facilitation of Ba^{2+} currents through $Ca_v2.2a$ was observed in the absence of G protein activation (Fig. 2*B*). After the prepulse to +100 mV, the voltage-dependent activation curve became steeper and was shifted from a V_a value of 36.1 ± 5.3 to 24.8 ± 1.5 mV (Fig. 2*B*). In addition, the maximum level of Ba^{2+} current attained during the 10-ms test pulse increased at the most positive test-pulse potentials, and the rate of activation accelerated 25-fold from a time constant of 17.1 ± 2.0 to 0.69 ± 0.02 ms (Fig. 2*B*).

Facilitation increases with more-positive prepulses for both $Ca_v2.1$ and $Ca_v2.2a$ (Fig. 2*C*). In fits with single Boltzmann equations, $Ca_v2.2a$ shows a higher maximum facilitation ratio of 4.61 ± 0.71 compared with a ratio of 1.52 ± 0.10 for $Ca_v2.1$. Half-maximal facilitation of $Ca_v2.1$ is observed at 65.1 ± 4.1 vs. 97.6 ± 19 mV for $Ca_v2.2a$, and the voltage dependence of facilitation is much steeper for $Ca_v2.1$ (k = 14.7 ± 2.5) vs. $Ca_v2.2a$ (k = 41.6 ± 2.8; Fig. 2*C*).

Rates of Onset and Reversal of Prepulse Facilitation. The influence of prepulse duration on facilitation was examined by varying the length of the prepulse between 1 and 1,000 ms. For both channel types, the facilitation ratio increases, reaches a plateau, and then decreases with increasing duration of the prepulse (Fig. 3*A*). The form of these curves reflects the interaction of three processes: the rate of facilitation, the rate of reversal of facilitation, and the rate of inactivation during the prepulse. The rate of facilitation is 3-fold slower for $Ca_v2.2a$ (τ = 15.4 ± 0.9 ms) than for $Ca_v2.1$

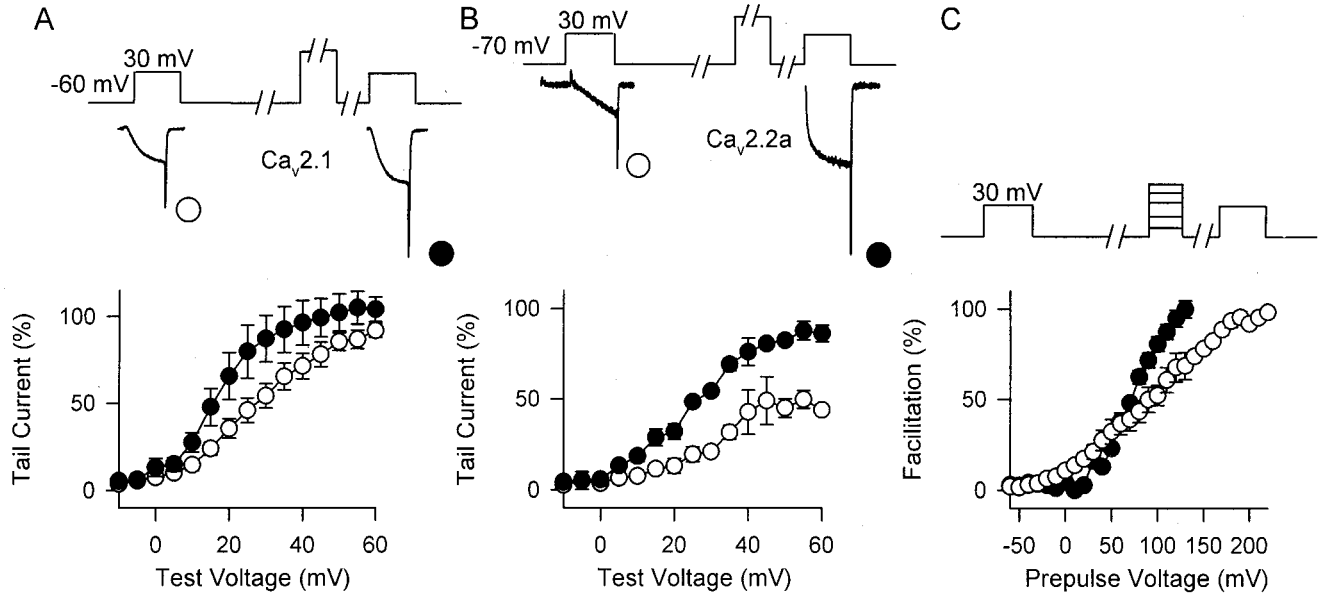

Fig. 2. Facilitation of $Ca_v2.1$ and $Ca_v2.2a$. (*A*) Prepulse facilitation of $Ca_v2.1$ channels. A 4-ms test pulse (test 1) to the indicated test potential was applied from the holding potential of −60 mV. After 1 s, a 10-ms conditioning prepulse to +100 mV was applied, the cell was repolarized to −60 mV for 10 ms, and a second 4-ms test pulse (test 2) identical to test-pulse 1 was applied. Means ± SEM of Ba^{2+} tail currents were plotted against test-pulse potentials. ○, test 1; ●, test 2. (*B*) Prepulse facilitation of $Ca_v2.2a$ channels. As in *A*, except 10-ms test pulses were used, and the repolarization was for 1 ms to −70 mV. ○, test 1; ●, test 2. Current traces shown above *A* and *B* were recorded during and after test 1 and test 2 at +30 mV. (*C*) Voltage dependence of facilitation. A 4-ms (α_1) or 10-ms ($Ca_v2.2a$) test pulse to +30 mV was applied from the holding potential of −60 mV ($Ca_v2.1$) or −70 mV ($Ca_v2.2a$). After 1 s, a 10-ms conditioning prepulse to the indicated potential was applied, the cell was repolarized to −60 mV ($Ca_v2.1$) for 10 ms or −70 mV ($Ca_v2.2a$) for 1 ms, and a second 4-ms ($Ca_v2.1$) or 10-ms ($Ca_v2.2a$) test pulse (test 2) to +30 mV was applied. Peak tail currents following each test pulse were measured. The facilitation ratio was calculated by dividing currents in test 2 by the currents in test 1, and means ± SEM of normalized facilitation ratios were plotted against the conditioning pulse potential. ●, $Ca_v2.1$; ○, $Ca_v2.2a$.

(τ = 4.8 ± 0.4 ms; Fig. 3*B*). Little facilitation of $Ca_v2.1$ is observed in the absence of GTPγS, and the Ba^{2+} current is depressed below the unfacilitated level for $Ca_v2.1$ and $Ca_v2.2a$ during long prepulses (Fig. 3*A*) because of voltage-dependent inactivation. During single depolarizing pulses, the activity of $Ca_v2.2a$ is inactivated with a time constant of 132 ± 26 ms at +100 mV vs. 462 ± 254 ms for $Ca_v2.1$ (Fig. 3*C*). Likewise, loss of facilitation after a prepulse is also much faster for $Ca_v2.2a$ with a time constant of 4.5 ± 1.0 ms compared with $Ca_v2.1$ with a time constant of 51.3 ± 7.3 ms (Fig. 3*D*).

Regulation by PKC. PKC has direct regulatory effects on N-type and P/Q-type Ca^{2+} channels in neurons (29) and also reverses their inhibition by neurotransmitters acting through G protein-coupled receptors (30, 31). Activation of PKC with OAG shifts the voltage dependence of activation of $Ca_v2.1$ in the presence of GTPγS from a midpoint of 33.3 ± 2.7 mV to a midpoint of 13.4 ± 1.8 mV (Fig. 4*A*), which completely reverses the effect of G protein activation and occludes voltage-dependent facilitation (Fig. 4*A*).

Because activation of $Ca_v2.2a$ is not altered by GTPγS, we analyzed the effect of the PKC activator by using the control intracellular solution. Under these conditions, OAG shifted the voltage dependence of activation from a V_a of 42.2 ± 1.1 to 37.3 ± 2.3 mV (Fig. 4*B*). Prepulse facilitation of $Ca_v2.2a$ also was diminished significantly, although substantial facilitation remained. After activation of PKC with OAG, the activation curves for $Ca_v2.2a$ channels before and after prepulse facilitation approached the same maximum (Fig. 4*B*) unlike the increase in maximum current observed with facilitation under control conditions (Fig. 2*B*). Thus, the intrinsic facilitation of α_1 is inhibited by activation of PKC in a similar manner to the G protein-dependent facilitation of $Ca_v2.1$, but the inhibition is less complete.

Stimulation of PKC by OAG also accelerated inactivation for both channel types (Fig. 4 *C* and *D*). The time constant for inactivation at +30 mV was decreased from 127 ± 24 to 49 ± 16 ms for $Ca_v2.1$ and from 313 ± 28 to 115 ± 17 ms for $Ca_v2.2a$. A similar increase in inactivation rate was observed for test potentials from 15 to 35 mV. In addition, the midpoint for steady-state inactivation was shifted from −25.4 ± 2.2 to −47.5 ± 1.3 mV for $Ca_v2.1$ (Fig. 4*C*) and from −41.5 ± 0.42 to −55.2 ± 3.4 mV for $Ca_v2.2a$ (Fig. 4*D*).

All the effects of OAG could be reversed by the PKC-IP in the pipette solution (Fig. 4). These results confirm the specificity of the effects of OAG and support the conclusion that phosphorylation by PKC alters activation, inactivation, voltage-dependent facilitation, and G protein modulation.

Effects of Ca^{2+}-Channel β Subunits. Caβ subunits influence Ca_v2 channel voltage dependence, prepulse facilitation, and modulation by G proteins (2, 40–43). Therefore, we examined key features of modulation of the $Ca_v2.1$ channel by G proteins in the absence of Caβ subunits, as well as in the presence of a different Caβ subunit, $Ca\beta_3$ (44). Unfortunately, currents conducted by expressed $\alpha_1 2.2a$ alone were too small to measure reliably.

In the presence of $Ca\beta_{1b}$ or $Ca\beta_3$ subunits, whole-cell currents increased 6.5-fold from −101 ± 21 pA (n = 11) for $\alpha_1 2.1$ subunits alone to −660 ± 120 pA ($Ca\beta_{1b}$; n = 28) or −667 ± 235 pA ($Ca\beta_3$; n = 21), as for expression in *Xenopus* oocytes (8, 45). The voltage dependence of activation was similar for cells coexpressing either the $Ca\beta_{1b}$ or $Ca\beta_3$ subunits (Fig. 5*A*) ($Ca\beta_{1b}$, V_a = 23.6 ± 1.4 mV; $Ca\beta_3$, V_a = 22.0 ± 0.3 mV). However, activation curves from cells expressing the $\alpha_1 2.1$ subunit alone had a more-positive voltage dependence (Fig. 5*A*; V_a = 30.4 ± 1.6 mV).

Coexpression of Caβ subunits also had substantial effects on inactivation. The time constant for inactivation of open channels during a depolarization to +15 mV decreased from 237 ±

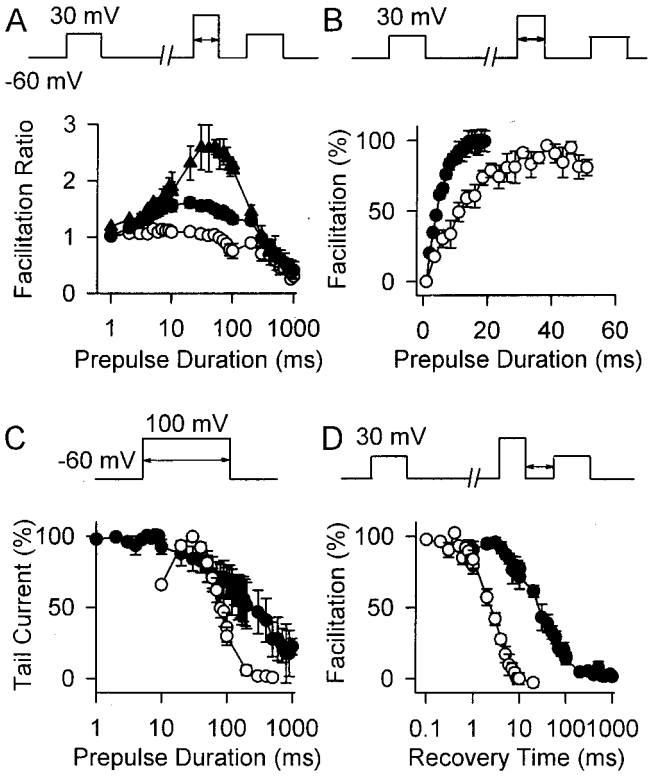

Fig. 3. Rates of onset and reversal of prepulse facilitation. (*A*) Time course of prepulse facilitation and inactivation. Facilitation was measured as in Fig. 2 *A* and *C* with prepulses of the indicated durations for $Ca_v2.1$, control (○), GTPγS (●). ▲, $Ca_v2.2a$. (*B*) Rate of onset of prepulse facilitation. Facilitation was measured as in Fig. 2 *A* and *C* with prepulses of the indicated durations. ●, $Ca_v2.1$ with GTPγS; ○, $Ca_v2.2a$, control. (*C*) Rates of inactivation. Inactivation was measured as in Fig. 1*B* by using prepulses of the indicated durations to +100 mV. ●, $Ca_v2.1$; ○, $Ca_v2.2a$. (*D*) Rates of reversal of prepulse facilitation. Facilitation was measured as in Fig. 2 *A* and *B* with a prepulse to +30 mV and repolarization for the indicated time periods before test-pulse 2. ●, $Ca_v2.1$; ○, $Ca_v2.2a$.

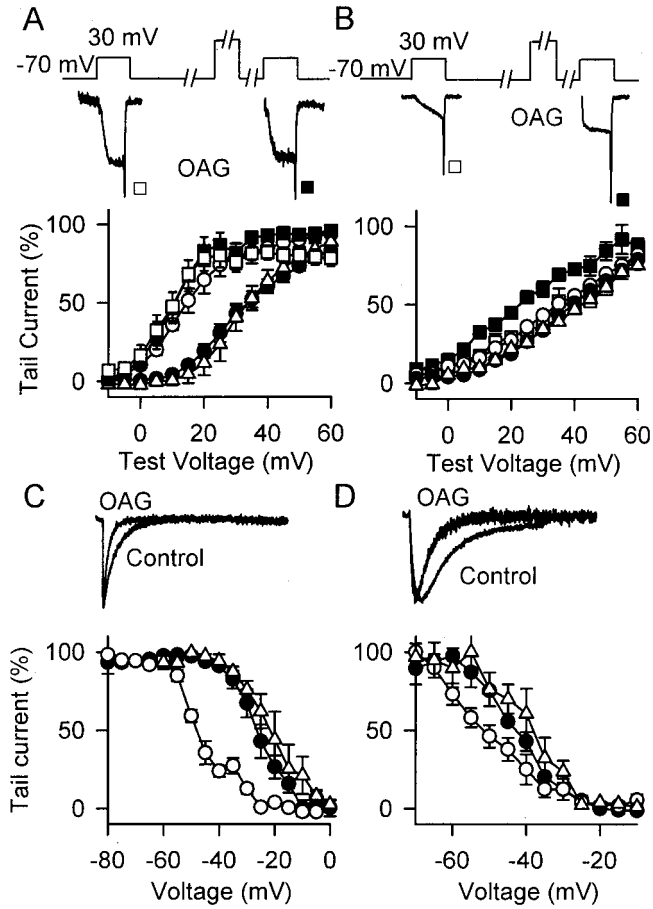

Fig. 4. Influence of PKC on Ca^{2+}-channel gating and modulation. (*A* and *B*) Voltage dependence of activation and facilitation were measured as in Fig. 1 with and without treatment with OAG. (*A*) $Ca_v2.1$. Activation: ●, GTPγS; ○, GTPγS plus OAG; △, PKC-inhibitor peptide (IP). Facilitation: □, GTPγS plus OAG test 1; ■, GTPγS plus OAG test 2. (*B*) Cav2.2a. ●, no addition; ○, OAG; △, OAG + PKC-IP. Facilitation: □, OAG test 1; ■, OAG test 2. (*C* and *D*) Influence of PKC on inactivation. Voltage dependence of inactivation was measured as in Fig. 1 in the presence and absence of OAG. (*C*) $Ca_v2.1$: ○, OAG; ●, GTPγS; △, PKC-IP. (*D*) $Ca_v2.2a$: ○, OAG; ●, GTPγS; △, PKC-IP.

29 ms (n = 3) to 110 ± 14 ms for $Ca\beta_{1b}$ and 88 ± 12 ms for $Ca\beta_3$ (Fig. 5*B*), with less pronounced effects for stronger depolarizations. In contrast, the presence of Caβ subunits had little effect on the voltage dependence of steady-state inactivation (data not shown). Overall, expressing $\alpha_1 2.1$ subunits in the absence of Caβ subunits reduces current amplitude, shifts the voltage dependence of activation toward more positive potentials, and slows the rates of activation and inactivation. The resulting channels in their unmodulated state are similar to $\alpha_1 2.1\beta_{1b}$ channels modulated by G proteins or $Ca_v2.2a$ channels under basal conditions.

Effects of $Ca_v\beta$ Subunits on G Protein Modulation and Prepulse Facilitation. For channels containing $\alpha_1 2.1$ and $Ca\beta_3$ subunits, V_a shifted from 22.0 ± 0.3 mV to 33.8 ± 2.3 mV when the pipette solution contained GTPγS (Fig. 5*C*) as for channels with β_{1b} subunits. In contrast, the positively shifted voltage dependence of channels containing $\alpha_1 2.1$ alone was affected little by GTPγS (Fig. 5*D*). This finding is consistent with the idea that channels having only $\alpha_1 2.1$ subunits cannot be modulated by G proteins because they are already in the *R* state. Coexpression of $\alpha_1 2.1$ subunits with β_{1b} subunits (Fig. 5*E*) or β_3 subunits (not shown) resulted in prepulse facilitation over a broad range of test-pulse voltages. However, when $\alpha_1 2.1$ was expressed without β subunits, there was little facilitation, even in the presence of intracellular GTPγS (Fig. 5*F*). Thus, although $\alpha_1 2.1$ expressed alone resembles $Ca_v2.2a$ in its kinetic properties and its failure to be modulated by GTPγS, it differs in being affected little by prepulse facilitation protocols under any condition tested. These results are consistent with the idea that Caβ subunits are required for $\alpha_1 2.1$ to enter the *W* state.

Discussion

An Allosteric Model of G Protein Modulation. G protein modulation of N-type Ca^{2+} channels is thought to shift them from a state in which activation is easier (*W*) to a state in which activation is slower and more difficult (*R*; ref. 16). The *W* and *R* states are thought to be intrinsic states of the Ca^{2+} channel, and G protein activation is thought to modulate the equilibrium between these states (16), but no direct evidence that the *W* and *R* states are intrinsic to the Ca^{2+} channel has been presented. The effect of G proteins is mediated by the Gβγ subunits (23, 24) through direct binding to site(s) in the α_1 subunits (25–28). Extending the original model of Bean (16) to include binding of Gβγ subunits, G protein regulation can be considered as a cyclic allosteric regulation of Ca^{2+}-channel functional state by binding of Gβγ as follows:

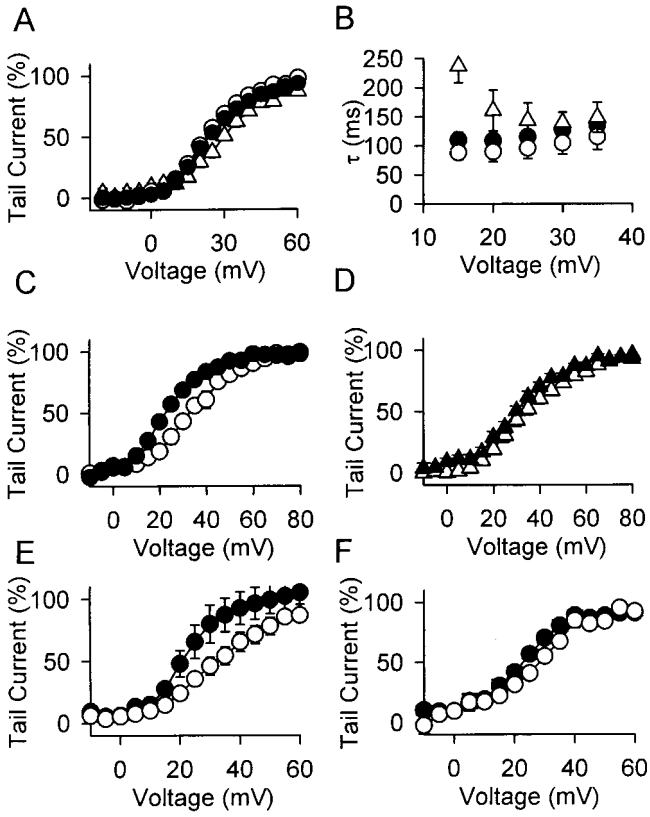

Fig. 5. Effects of $Ca_v\beta$ subunits on properties of $Ca_v2.1$ Ca^{2+} channels. $Ca_v2.1$ and $\alpha_2\delta$ subunits were expressed without (△) or with Ca^{2+}-channel β_{1b} (●) or β_3 (○) subunits in tsA-201 cells. (*A*) Voltage dependence of activation and inactivation measured as in Fig. 1. (*B*) Time constants of inactivation determined during 1,000-ms long test pulses to the indicated potentials. (*C*) $Ca_v2.1$ and $\alpha_2\delta$ subunits were expressed with Ca^{2+}-channel β_3 subunits and studied in the presence (○) or absence (●) of intracellular GTPγS. (*D*) $Ca_v2.1$ and $\alpha_2\delta$ subunits were expressed and studied in the presence (△) or absence (▲) of GTPγS. (*E* and *F*) Activation curves recorded with intracellular GTPγS in the absence (○) and presence (●) of a preceding conditioning prepulse as described for Fig. 1 from cells coexpressing $\alpha_1 2.1$, $\alpha_2\delta$, and $Ca\beta_{1b}$ (*E*) or $\alpha_1 2.1$ and $\alpha_2\delta$ alone (*F*).

$$\begin{array}{ccc} W + G\beta\gamma & \overset{K_W}{\rightleftharpoons} & W{\cdot}G\beta\gamma \\ K_{WR}(V) \quad \uparrow\downarrow & & \uparrow\downarrow \\ R + G\beta\gamma & \underset{K_R}{\rightleftharpoons} & R{\cdot}G\beta\gamma \end{array} \qquad [1]$$

Activation from both the *W* and *R* states after depolarization involves voltage-dependent transitions through a series of closed states to an open state (46) accompanied by outward movement of gating charge at each step (47). For the *R* state, the initial voltage-dependent transitions to neighboring closed states or to the *W* state are slow (47), resulting in the reluctant gating mode.

This model is derived directly from the allosteric model of Monod *et al.* (48) and is similar in form to models used for neurotoxin activation of sodium channels (49) and block of sodium channels by local anesthetics (the "modulated receptor hypothesis"; ref. 50). The fraction of channels in the *R* state is controlled by the equilibrium constant (K_{WR}) for the transition from *R* to *W*, the binding constants for $G\beta\gamma$ to the *W* and *R* states, and the concentration of activated $G\beta\gamma$ according to the following equation:

$$F_R = \frac{1}{1 + K_{WR}\dfrac{1 + [G\beta\gamma]/K_W}{1 + [G\beta\gamma]/K_R}} \qquad [2]$$

There are not enough quantitative data on intracellular G protein concentrations, G protein binding affinity, and voltage-dependent Ca^{2+}-channel modulation to fit the parameters of this model objectively. However, our results for the different modulators studied here are qualitatively consistent with this model with two assumptions: (*i*) K_{WR} is smaller for certain channel types such that they are tonically in the *R* state in the absence of G protein modulation; and (*ii*) each modulator allosterically alters K_{WR} as a primary mechanism of action.

Different Values for K_{WR} Account for Differences in Channel Modulation. When expressed with Ca^{2+}-channel β subunits, $Ca_v2.1$ activates at much more negative membrane potentials than $Ca_v2.2a$ (Fig. 1), and its voltage dependence of activation is shifted to more positive membrane potentials by activation of G proteins. In contrast, $Ca_v2.2a$ expressed with β subunits and $Ca_v2.1$ expressed without β subunits activate at more positive membrane potentials, and their voltage dependence of activation is unaffected by G protein activation or inhibition. These results are consistent with the conclusion that K_{WR} is much smaller for these channels under our experimental conditions, causing most of these channels to be in the *R* state without G protein activation.

G Protein Activation Shifts $\alpha_1 2.1\beta$ to the *R* State, Whereas $\alpha_1 2.1$ and $\alpha_1 2.2a\beta$ Are Intrinsically in the *R* State. In this model, activation of G proteins with GTPγS shifts $\alpha_1 2.1\beta$ to the *R* state and thereby shifts its voltage dependence of activation to more positive membrane potentials and slows its activation. In contrast, activation of G proteins with GTPγS has no effect on $\alpha_1 2.1$ alone or on $\alpha_1 2.2a\beta$ because all of the channels are in the *R* state, and no further shift can be caused by $G\beta\gamma$. Inhibition of G proteins by GDPβS or *N*-ethyl maleimide also has no effect on facilitation of $\alpha_1 2.2a$, even though the heterotrimeric form of the G protein induced by GDPβS or *N*-ethyl maleimide is inactive in signal transduction. These results provide evidence that a Ca^{2+} channel can adopt the *R* state without G protein activation and therefore directly support the idea that the *W* and *R* states are intrinsic functional states of the Ca^{2+} channel.

Prepulse Facilitation Shifts $\alpha_1 2.1\beta$ and $\alpha_1 2.2a\beta$ to the *W* State but Has a Smaller Effect on $\alpha_1 2.1$. In the context of this model, the effect of strong depolarizing prepulses is viewed as a voltage-dependent increase in the value of K_{WR}. This increase is large enough to shift $\alpha_1 2.1\beta$ channels toward the *W* state even in the presence of activated G proteins. The voltage-dependent increase in K_{WR} is also large enough to shift $\alpha_1 2.2a$ to the *W* state, and thus prepulse facilitation is observed in the absence of G protein modulation. However, it is not large enough to cause substantial facilitation of channels containing $\alpha_1 2.1$ without $Ca\beta$ subunits. The results with $\alpha_1 2.2a$ provide the first evidence that prepulse facilitation is intrinsic to the Ca^{2+} channel itself and can occur without G protein modulation. The results with coexpression of $Ca\beta$ subunits provide evidence that they can act by shifting channels from the *R* to the *W* state.

Phosphorylation by PKC Shifts Both $\alpha_1 2.1\beta$ and $\alpha_1 2.2a\beta$ to the *W* State. Previous work shows that activation of PKC in neurons can increase Ca^{2+}-channel activity directly (29) and also can reverse G protein inhibition and thereby increase Ca^{2+}-

channel activity indirectly (30, 31). Our results show that these two seemingly independent effects of PKC can be considered as two manifestations of the same intrinsic regulatory mechanism. For $\alpha_1 2.1\beta$ Ca^{2+} channels, G protein modulation is required to shift Ca^{2+} channels to the *R* state, and activation of PKC can shift them back toward the *W* state and thereby facilitate Ca^{2+}-channel activation. For $\alpha_1 2.2a\beta$ channels, PKC can act directly because these channels are already in the *R* state without G protein activation and can be shifted back to *W* by phosphorylation. These results implicate the Ca^{2+} channel α_1 subunits as the sites of phosphorylation that cause this regulatory effect of PKC, which is in agreement with results identifying required PKC phosphorylation sites in the intracellular loop connecting domains I and II (27).

Caβ Subunits Also Shift Ca^{2+} Channels to the *W* State. Numerous studies have shown that coexpression of Caβ subunits shifts the voltage dependence of activation of Ca^{2+} channels containing $\alpha_1 2.1$ and $\alpha_1 2.2$ subunits to more negative potentials (2, 34, 40, 41, 45). Our results show that $\alpha_1 2.1$ expressed alone is tonically in the *R* state and that coexpression of Caβ subunits shifts it to the *W* state. Thus, one functional effect of Caβ subunits is to shift channels to the willing gating mode. This effect of Caβ subunits is expected to oppose G protein modulation, as observed in both neurons and *Xenopus* oocytes (41–43). Paradoxically, although Caβ subunits oppose G protein modulation, we find that a Caβ subunit is required for G protein modulation of $\alpha_1 2.1$ (see also ref. 51). This surprising result is expected from the allosteric model of channel modulation because, if $\alpha_1 2.1$ expressed alone is tonically in the *R* state, G proteins cannot inhibit its activity further and therefore seem inactive. Thus, modulation of the equilibrium between the *W* and *R* states is important for the effects of G proteins, PKC, and Caβ subunits.

Subtypes of N-type and P/Q-type Ca^{2+} Channels. Multiple molecular isoforms of N-type and P/Q-type Ca^{2+}-channel α_1 subunits have been identified. Our experiments compare the properties of two specific molecular isoforms, the $Ca_v 2.2a$ isoform of N-type channels, and the $Ca_v 2.1$ isoform of P/Q-type channels. The regulatory properties of $Ca_v 2.2a$ described here differ significantly from the properties of $Ca_v 2.2b$ described previously (32, 52). $Ca_v 2.2b$ channels activate more rapidly and at more negative membrane potentials than the $Ca_v 2.2a$ channels studied here, and G protein activation is required to observe voltage-dependent facilitation. Thus, it is likely that the $Ca_v 2.2b$ isoform is tonically primarily in the *W* state while the $Ca_v 2.2a$ isoform is tonically in the *R* state. The following paper (37) identifies a single amino acid residue that specifies this difference in channel gating properties.

We thank Drs. Charles Chavkin and Kenneth Mackie for comments on a draft of the manuscript. This work was supported by Research Grant NS22625 from the National Institutes of Health to W.A.C. and a postdoctoral fellowship from the Deutsche Forschungsgemeinschaft to S.H.

1. Zhang, J.-F., Randall, A. D., Ellinor, P. T., Horne, W. A., Sather, W. A., Tanabe, T., Schwarz, T. L. & Tsien, R. W. (1993) *Neuropharmacology* **32,** 1075–1088.
2. Hofmann, F., Biel, M. & Flockerzi, V. (1994) *Annu. Rev. Neurosci.* **17,** 399–418.
3. Catterall, W. A. (1995) *Annu. Rev. Biochem.* **65,** 493–531.
4. Ertel, E. A., Campbell, K. P., Harpold, M. M., Hofmann, F., Mori, Y., Perez-Reyes, E., Schwartz, A., Snutch, T. P., Tanabe, T., Birnbaumer, L., *et al.* (2000) *Neuron* **25,** 533–535.
5. Dubel, S. J., Starr, T. V. B., Hell, J. W., Ahlijanian, M. K., Enyeart, J. J., Catterall, W. A. & Snutch, T. P. (1992) *Proc. Natl. Acad. Sci. USA* **89,** 5058–5062.
6. Williams, M. E., Feldman, D. H., McCue, A. F., Brenner, R., Velicelebi, G., Ellis, S. B. & Harpold, M. M. (1992) *Neuron* **8,** 71–84.
7. Mori, Y., Friedrich, T., Kim, M. S., Mikami, A., Nakai, J., Ruth, P., Bosse, E., Hofmann, F., Flockerzi, V., Furuichi, T., *et al.* (1991) *Nature (London)* **350,** 398–402.
8. Sather, W. A., Tanabe, T., Zhang, J. F., Mori, Y., Adams, M. E. & Tsien, R. W. (1993) *Neuron* **11,** 291–303.
9. Bourinet, E., Soong, T. W., Sutton, K., Slaymaker, S., Mathews, E., Monteil, A., Zamponi, G. W., Nargeot, J. & Snutch, T. P. (1999) *Nat. Neurosci.* **2,** 407–415.
10. Westenbroek, R. E., Sakurai, T., Elliott, E. M., Hell, J. W., Starr, T. V. B., Snutch, T. P. & Catterall, W. A. (1995) *J. Neurosci.* **15,** 6403–6418.
11. Cohen, M. W., Jones, O. T. & Angelides, K. J. (1991) *J. Neurosci.* **11,** 1032–1039.
12. Robitaille, R., Adler, E. M. & Charlton, M. P. (1990) *Neuron* **5,** 773–779.
13. Westenbroek, R. E., Hell, J. W., Warner, C., Dubel, S. J., Snutch, T. P. & Catterall, W. A. (1992) *Neuron* **9,** 1099–1115.
14. Tsien, R. W., Lipscombe, D., Madison, D. V., Bley, K. R. & Fox, A. P. (1988) *Trends Neurosci.* **11,** 431–438.
15. Dunlap, K., Luebke, J. I. & Turner, T. J. (1995) *Trends Neurosci.* **18,** 89–98.
16. Bean, B.P. (1989) *Nature (London)* **340,** 153–156.
17. Hille, B. (1994) *Trends Neurosci.* **17,** 531–536.
18. Dolphin, A. C. (1995) *Exp. Physiol.* **80,** 1–36.
19. Marchetti, C., Carbone, E. & Lux, H. D. (1986) *Pflügers Arch.* **406,** 104–111.
20. Tsunoo, A., Yoshii, M. & Narahashi, T. (1986) *Proc. Natl. Acad. Sci. USA* **83,** 9832–9836.
21. Elmslie, K. S., Zhou, W. & Jones, S. W. (1990) *Neuron* **5,** 75–80.
22. Ikeda, S. R. (1991) *J. Physiol. (London)* **439,** 181–214.
23. Ikeda, S. R. (1996) *Nature (London)* **380,** 255–258.
24. Herlitze, S., Garcia, D. E., Mackie, K., Hille, B., Scheuer, T. & Catterall, W. A. (1996) *Nature (London)* **380,** 258–262.
25. Page, K. M., Stephens, G. J., Berrow, N. S. & Dolphin, A. C. (1997) *J. Neurosci.* **17,** 1330–1338.
26. Herlitze, S., Hockerman, G. H., Scheuer, T. & Catterall, W. A. (1997) *Proc. Natl. Acad. Sci. USA* **94,** 1512–1516.
27. De Waard, M., Liu, H., Walker, D., Scott, V. E. S., Gurnett, C. A. & Campbell, K. P. (1997) *Nature (London)* **385,** 446–450.
28. Zamponi, G. W., Bourinet, E., Nelson, D., Nargeot, J. & Snutch, T. P. (1997) *Nature (London)* **385,** 442–446.
29. Yang, J. & Tsien, R. W. (1993) *Neuron* **10,** 127–136.
30. Swartz, K. J. (1993) *Neuron* **11,** 305–320.
31. Swartz, K. J., Merritt, A., Bean, B. P. & Lovinger, D. M. (1993) *Nature (London)* **361,** 165–168.
32. Stea, A., Soong, T.W. & Snutch, T. P. (1995) *Neuron* **15,** 929–940.
33. Starr, T. V. B., Prystay, W. & Snutch, T. P. (1991) *Proc. Natl. Acad. Sci. USA* **88,** 5621–5625.
34. Stea, A., Dubel, S. J., Pragnell, M., Leonard, J. P., Campbell, K. P. & Snutch, T. P. (1993) *Neuropharmacology* **32,** 1103–1116.
35. Ellis, S. B., Williams, M. E., Ways, N. R., Brenner, R., Sharp, A. H., Leung, A. T., Campbell, K. P., McKenna, E., Koch, W. J., Hui, A., *et al.* (1988) *Science* **241,** 1661–1664.
36. Margolskee, R. F., McHendry-Rinde, B. & Horn, R. (1993) *BioTechniques* **15,** 906–911.
37. Zhong, H., Li, B., Scheuer, T. & Catterall, W. A. (2001) *Proc. Natl. Acad. Sci. USA* **98,** 4705–4709.
38. Mintz, I. M. & Bean, B. P. (1993) *Neuron* **10,** 889–898.
39. Currie, K. P. M. & Fox, A. P. (1997) *J. Neurosci.* **17,** 4570–4579.
40. Berrow, N. S., Campbell, V., Fitzgerald, E. M., Brickley, K. & Dolphin, A. C. (1995) *J. Physiol. (London)* **482,** 481–491.
41. Campbell, V., Berrow, N. S., Fitzgerald, E. M., Brickley, K. & Dolphin, A. C. (1995) *J. Physiol. (London)* **485,** 365–372.
42. Bourinet, E., Soong, T. W., Stea, A. & Snutch, T. P. (1996) *Proc. Natl. Acad. Sci. USA* **93,** 1486–1491.
43. Roche, J. P., Anantharam, V. & Treistman, S. N. (1995) *FEBS Lett.* **371,** 43–46.
44. Castellano, A., Wei, X., Birnbaumer, L. & Perez-Reyes, E. (1993) *J. Biol. Chem.* **268,** 3450–3455.
45. De Waard, M. & Campbell, K. P. (1995) *J. Physiol. (London)* **485,** 619–634.
46. Boland, L. M. & Bean, B. P. (1993) *J. Neurosci.* **13,** 516–533.
47. Jones, L. P. Patil, P. G., Snutch, T. P. & Yue, D. T. (1997) *J. Physiol. (London)* **498,** 601–610.
48. Monod, J., Wyman, J. & Changeux, J.-P. (1965) *J. Mol. Biol.* **12,** 88–118.
49. Catterall, W. A. (1977) *J. Biol. Chem.* **252,** 8669–8676.
50. Hille, B. (1977) *J. Gen. Physiol.* **69,** 497–515.
51. Meir, A., Bell, D. C., Stephens, C. J., Page, K. M. & Dolphin, A. C. (2000) *Biophys. J.* **79,** 731–746.
52. Patil, P. G., deLeon, M., Reed, R. R., Dubel, S., Snutch, T. P. & Yue, D. T. (1996) *Biophys. J.* **71,** 2509–2521.